Supporting Information for

Two−Dimensional Inverse Double Sandwich CoB_7: Strain−Induced Non−magnetic to Ferromagnetic Transition

Liang Gu[§], Hui-Min Yang[§] and Li-Ming Yang*

Key Laboratory of Material Chemistry for Energy Conversion and Storage, Ministry of Education; Hubei Key Laboratory of Materials Chemistry and Service Failure; Hubei Key Laboratory of Bioinorganic Chemistry and Materia Medica; Hubei Engineering Research Center for Biomaterials and Medical Protective Materials; School of Chemistry and Chemical Engineering, Huazhong University of Science and Technology, Wuhan 430074, China. [§]*These authors contributed equally to the work. (email: Lmyang@hust.edu.cn)*

Table of Contents:

1. **Fig. S1**. (a) structural analysis, (b) relative energy, (c) phonon spectra, (d) AIMD simulation results, and (e) electronic properties of the low-lying CoB_7−i allotropes (i = 2, 3, 4, 6, 7). The relative energy is reference to that of the global minimum CoB_7−1.
2. **Fig. S2**. Phonon spectrum of the boron atomic layer in the CoB_7−1 structure with the Co atom removed.
3. **Fig. S3**. Charge density difference plot of the CoB_7−1 structure showing the distribution of electron density between the Co and B atoms.
4. **Fig. S4**. Calculated Bader charges of CoB_7−1, detailing the charge on each atom in the structure.
5. **Fig. S5**. Polar diagrams of in-plane Young's modulus Y(θ) and Poisson's ratio υ(θ) along different in-plane directions (θ) for eight low-lying CoB_7 allotropes.
6. **Fig. S6**. Phonon dispersion spectra of CoB_7−1 under biaxial strain (−2% to +10%) showing the stability range from −1% to +8%.
7. **Fig. S7**. Electronic band structures of CoB_7−1 under biaxial strain (−2% to +10%), illustrating changes in the electronic states near the Fermi level.
8. **Fig. S8**. Density of states (DOS) of CoB_7−1 under strain from +2% to +10%, highlighting the shift in electronic states under strain.
9. **Table S1**. Elastic constants (C_{ij}), layer modulus (γ), Young's modulus (Y), and Poisson's ratio (ν) for seven low-lying allotropes of 2D CoB_7 nanosheets (CoB_7−i, i=1−7), including a comparison with the ground state CoB_7−1.

CoB_7−2 (ΔE=37.0 meV, space group: *P*−*1*, No.2; unit cell: 16 atoms)

(a)

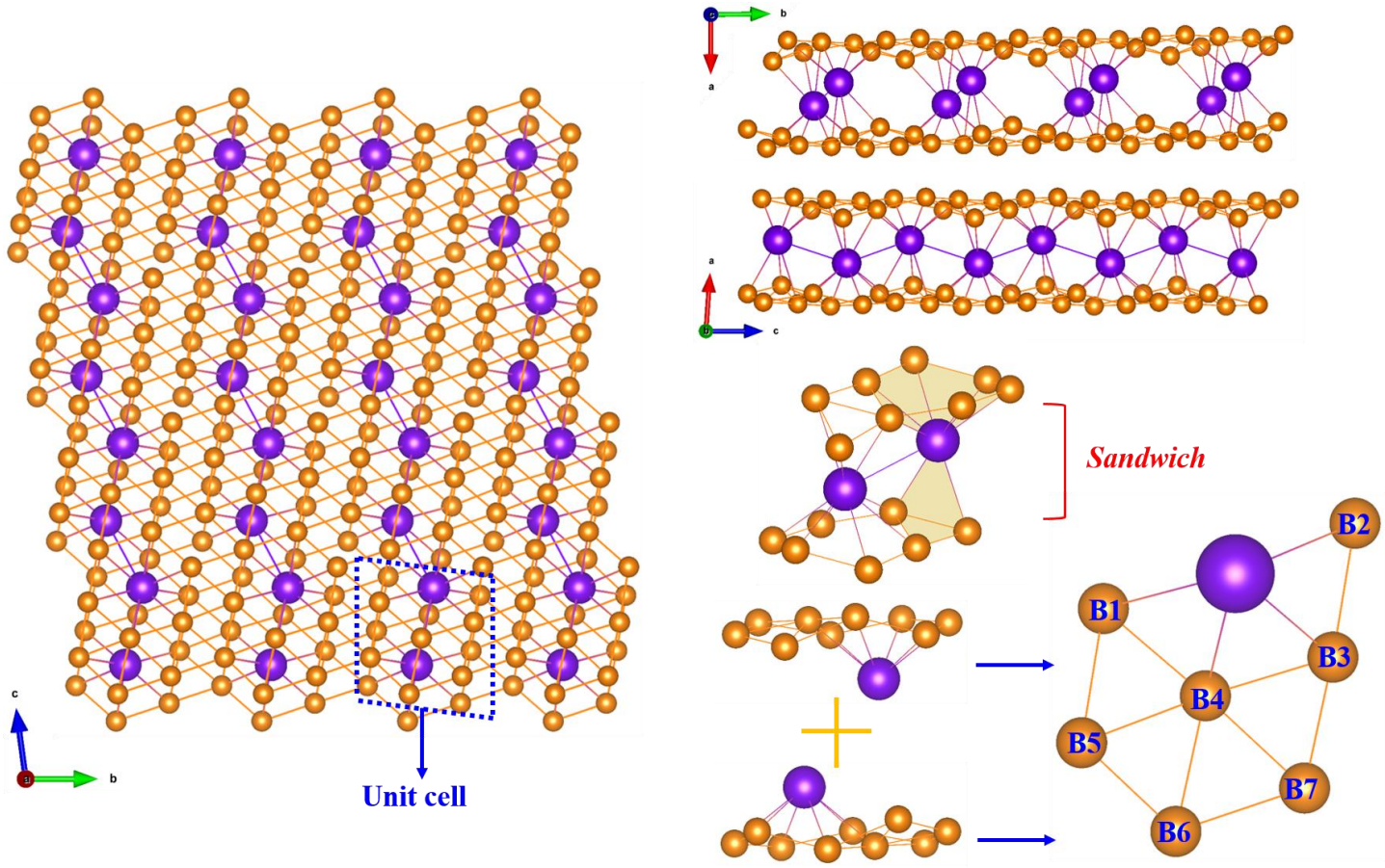

(b)

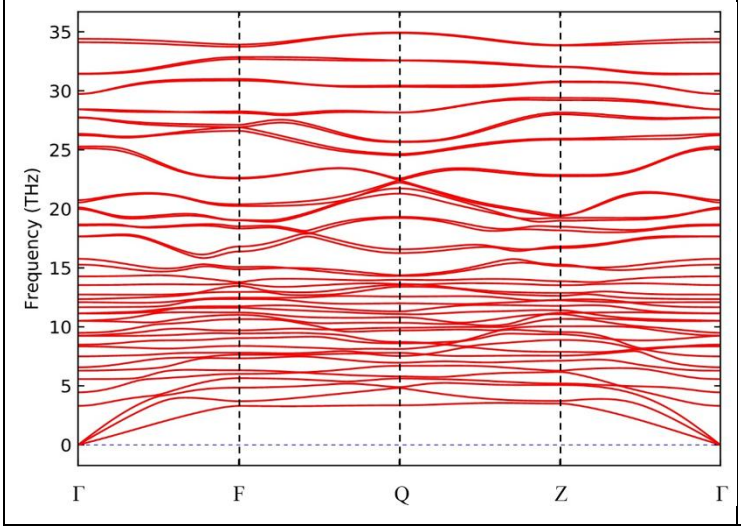

(c)

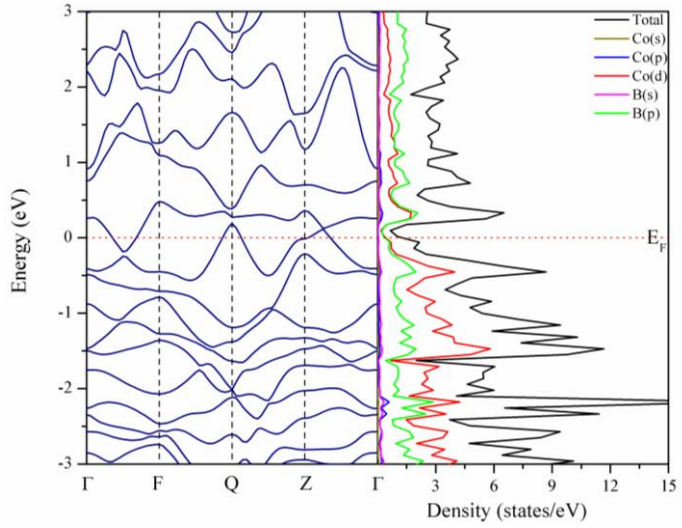

(d)

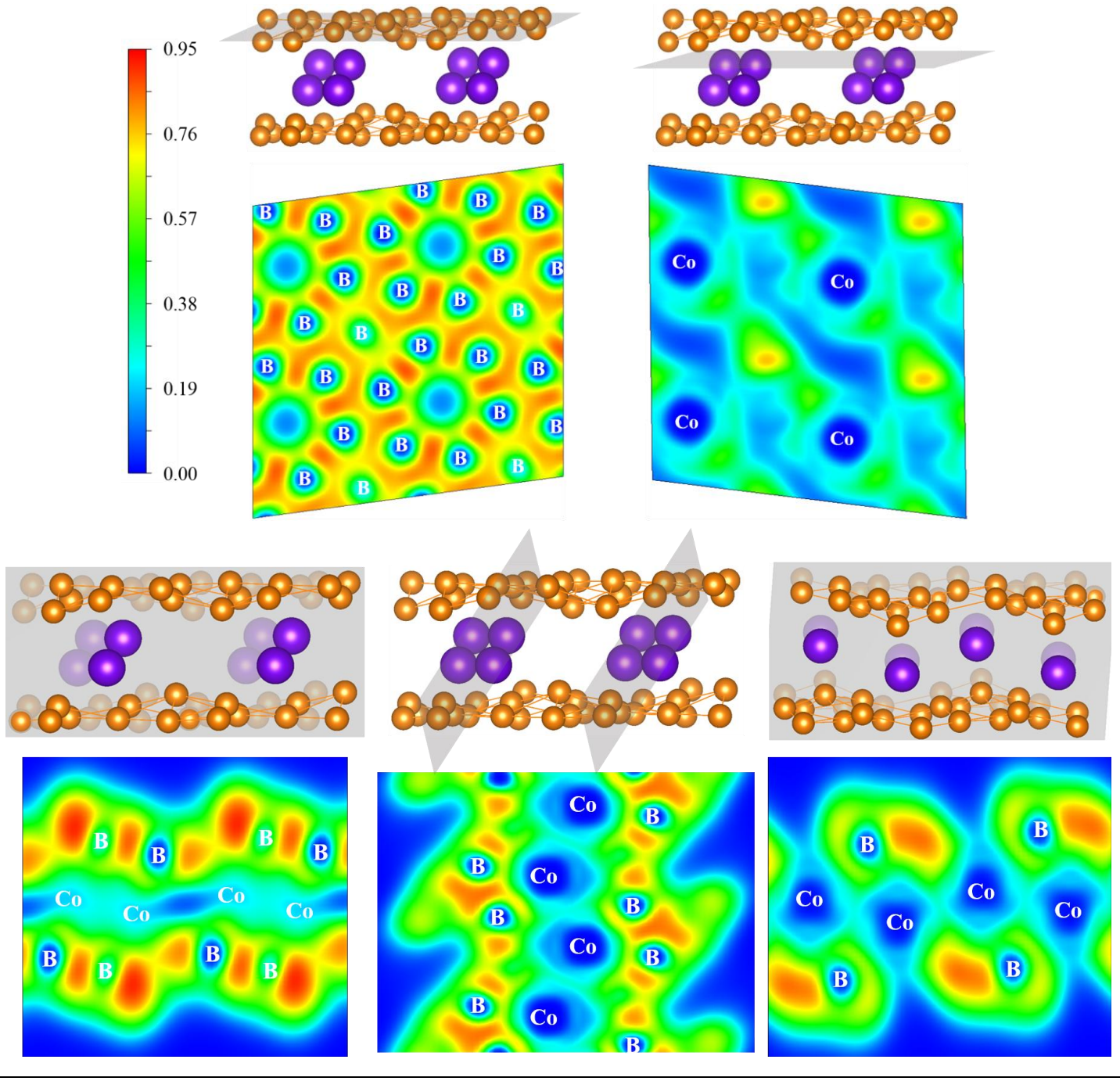
0.95
0.76
0.57
0.38
0.19
0.00
B
Co

(e)

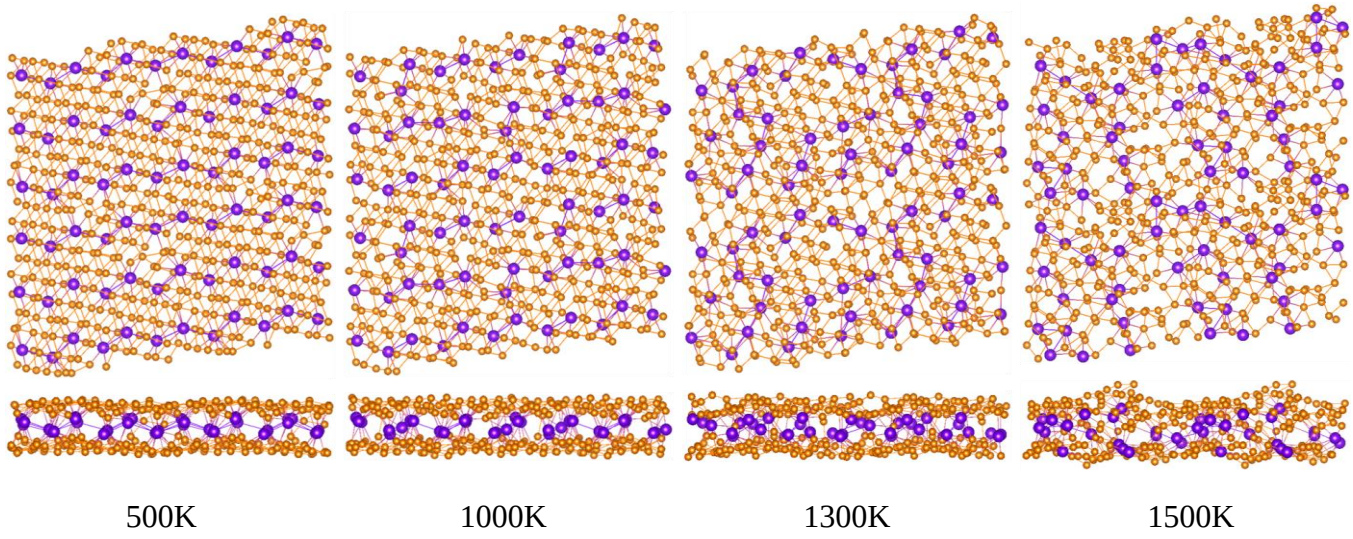
Top view
Side view
500K
1000K
1300K
1500K

CoB_7–3 (ΔE=37.1 meV, space group: *Pmm2*, No.25; unit cell: 16 atoms)

(a)

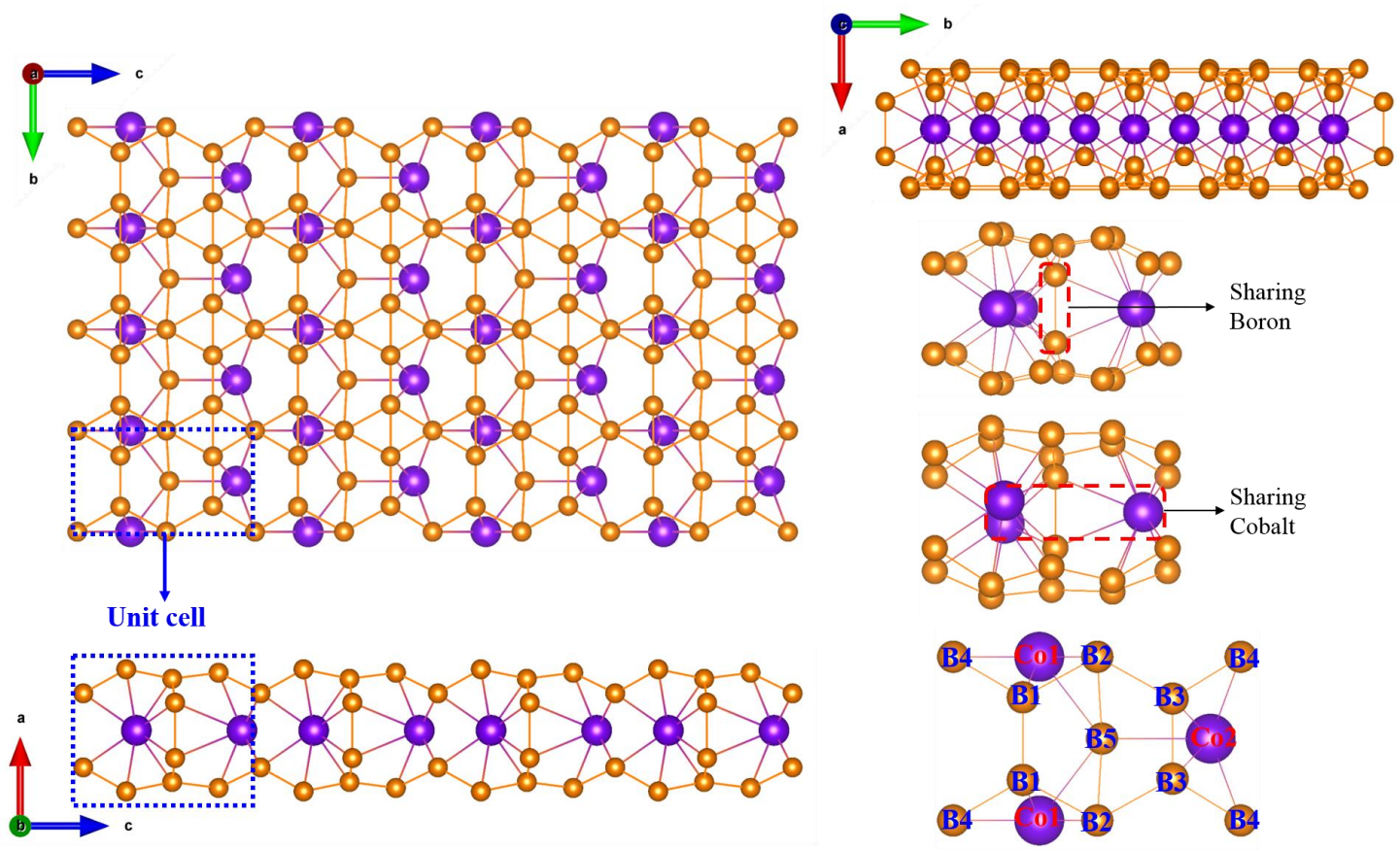

(b)

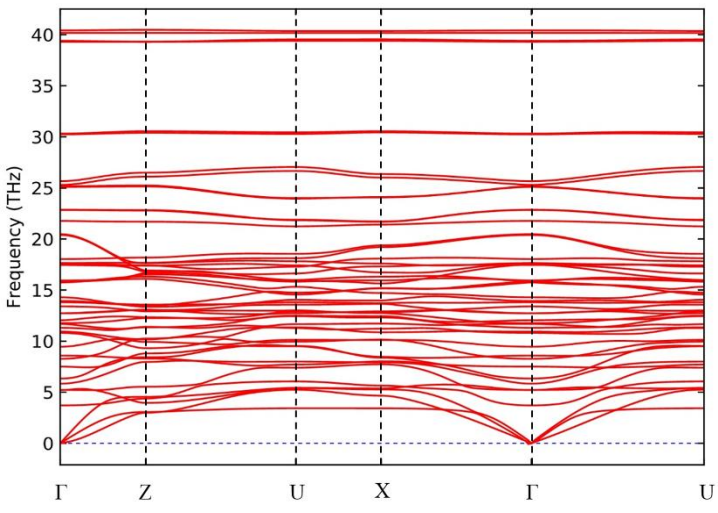

(c)

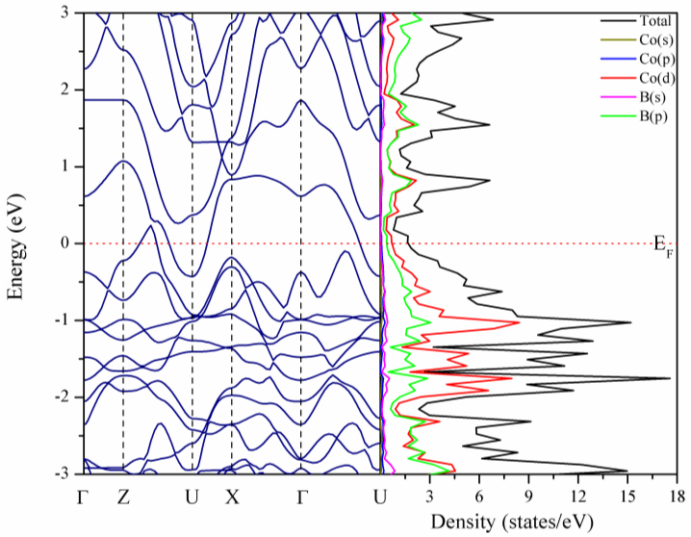

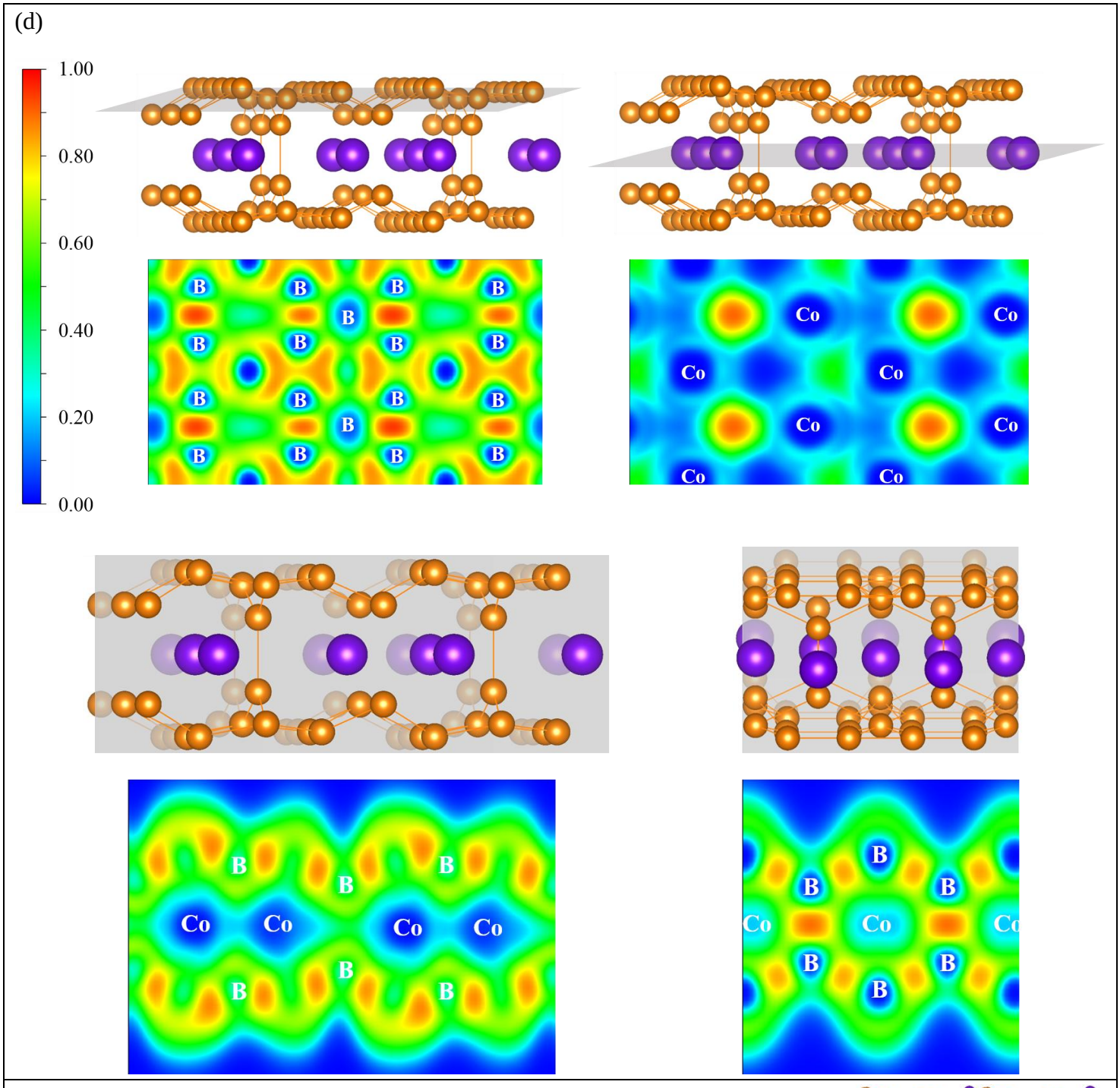
(d)
1.00
0.80
0.60
0.40
0.20
0.00
B
Co
(e)
Top view
Side view
500K
1000K
1300K
1500K

CoB_7–4 (ΔE=46.4 meV, space group: *P2/c*, No.13; unit cell: 16 atoms)

(a)

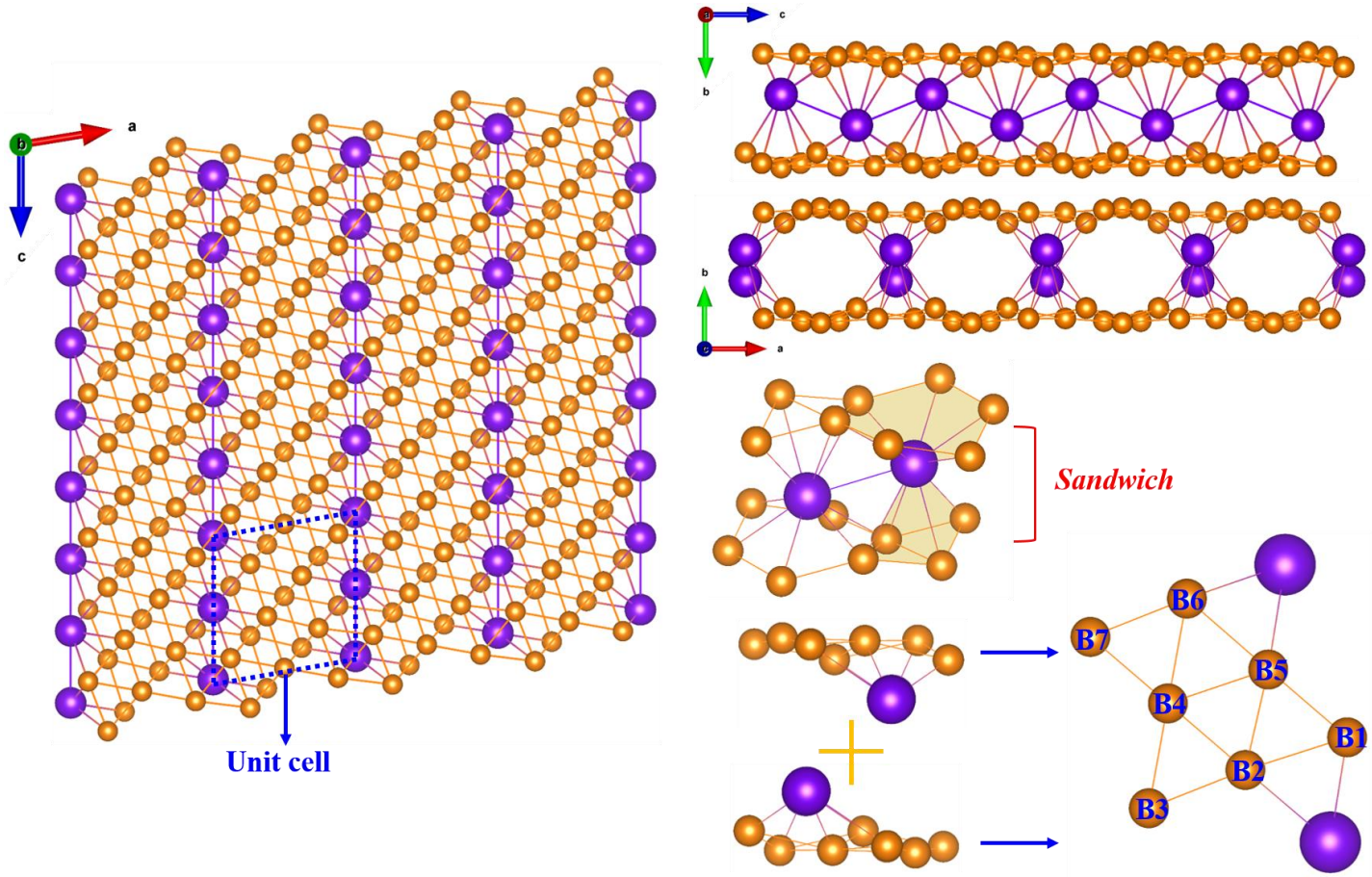

(b)

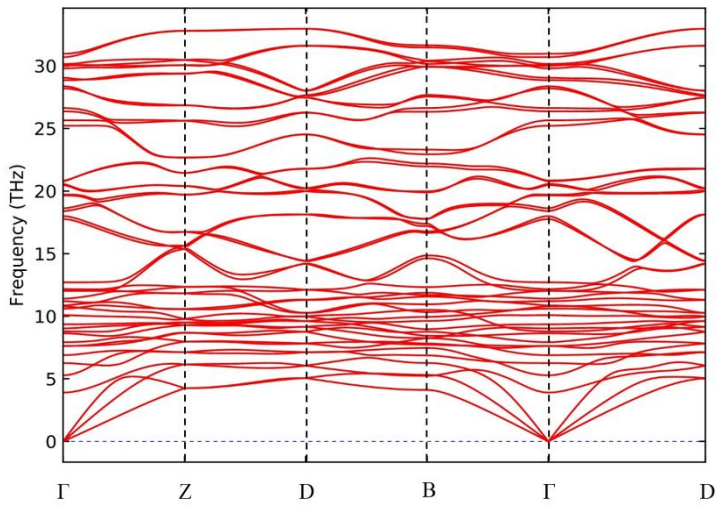

(c)

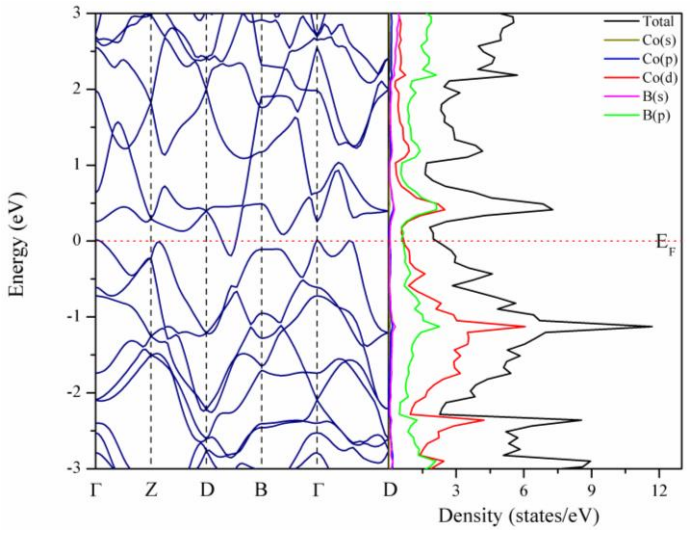

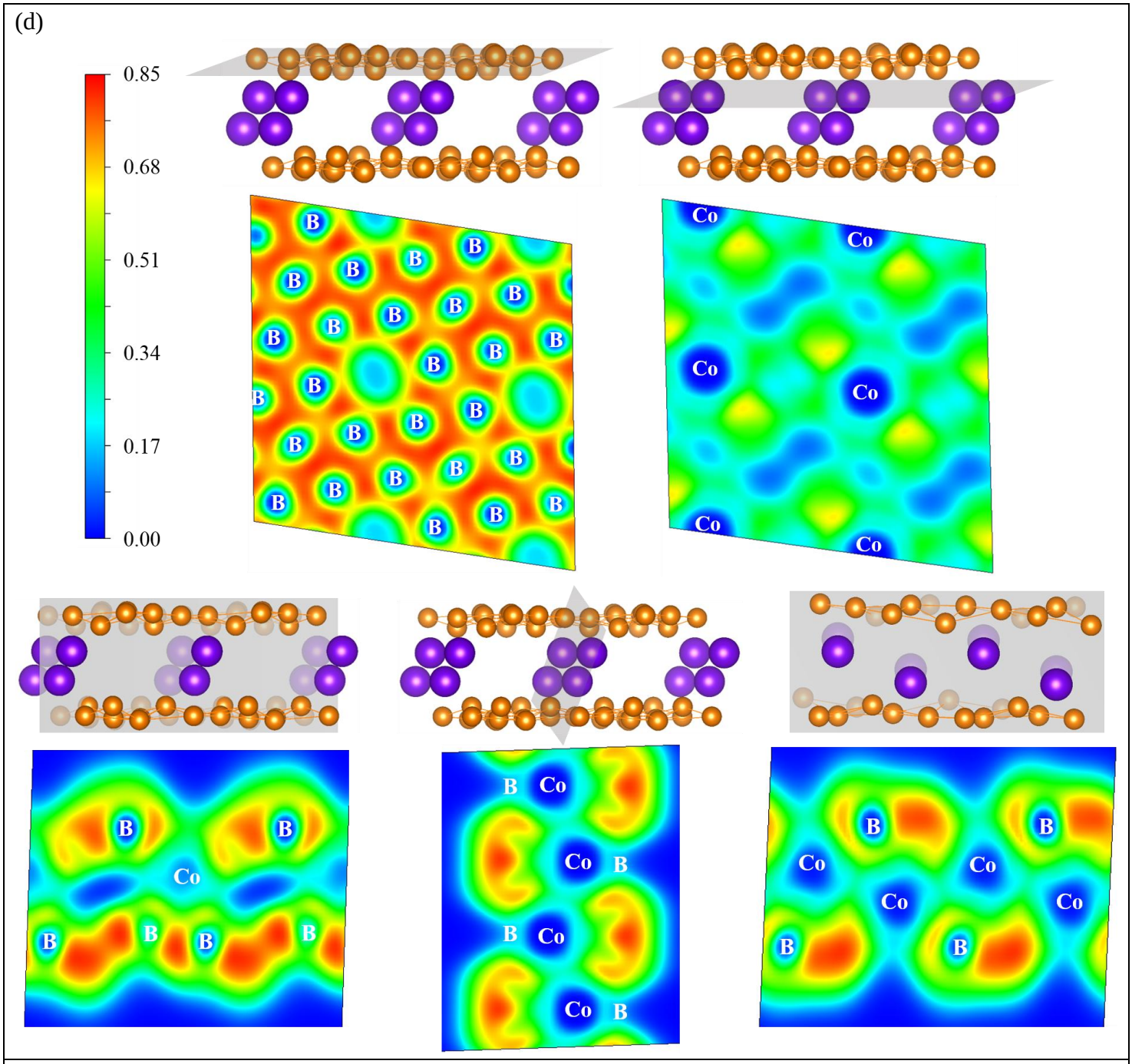
(d)
0.85
0.68
0.51
0.34
0.17
0.00
B
Co
(e)
Top view
Side view
500K
1000K
1300K
1500K

CoB_7−6 (ΔE=124.3 meV, space group: *P3m1*, No.156; unit cell: 8 atoms)

(a)

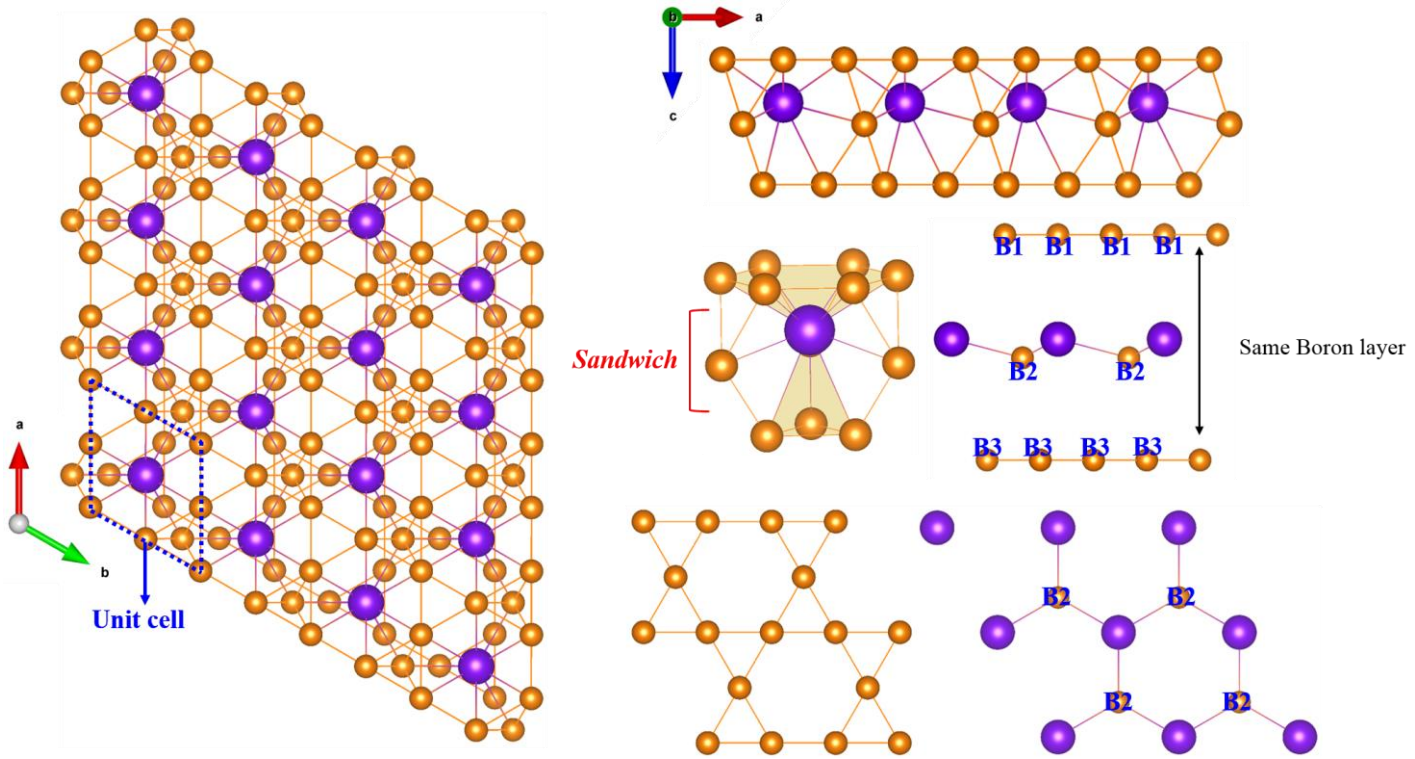

(b)

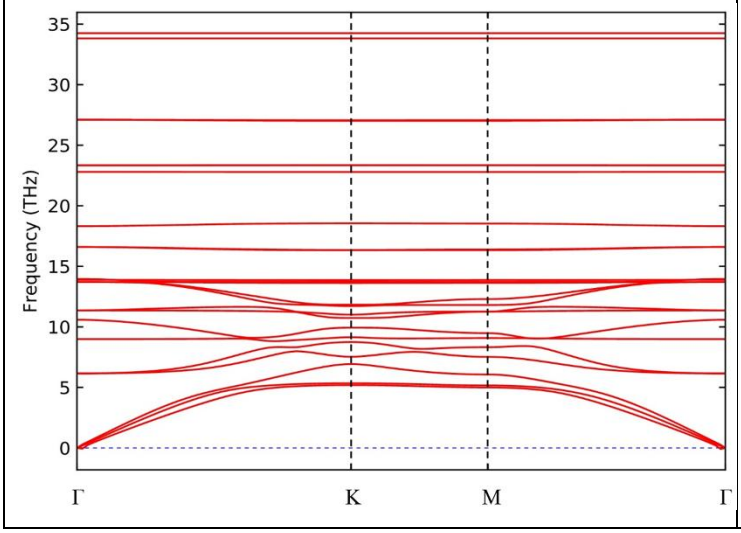

(c)

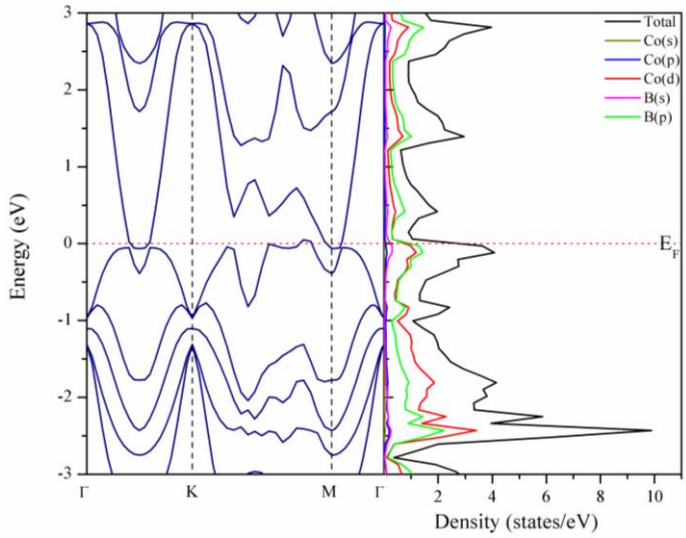

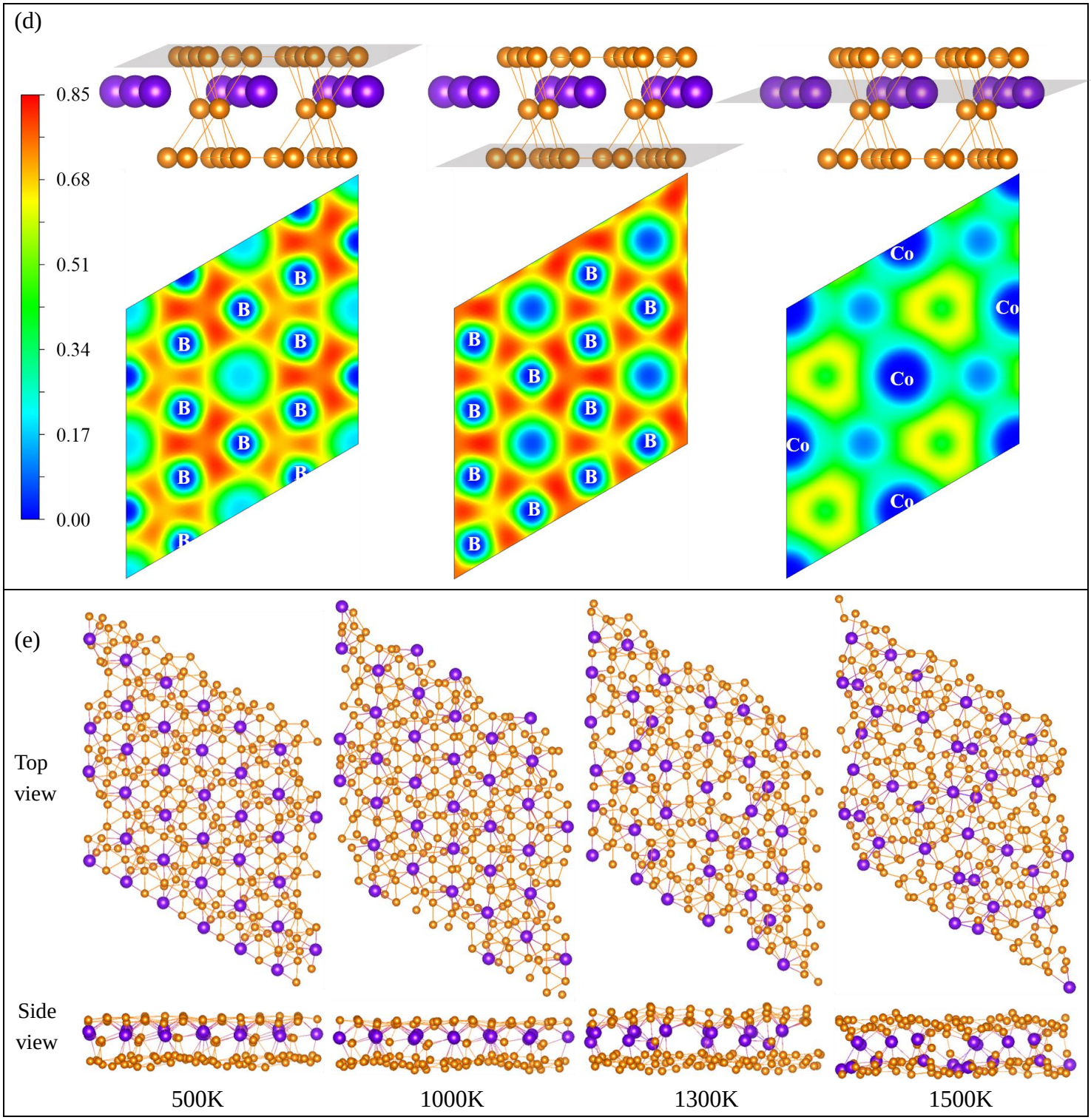
(d)
0.85
0.68
0.51
0.34
0.17
0.00
B
Co
(e)
Top view
Side view
500K
1000K
1300K
1500K

CoB_7–7 (ΔE=146.4 meV, space group: *Pm*, No.6; unit cell: 8 atoms)

(a)

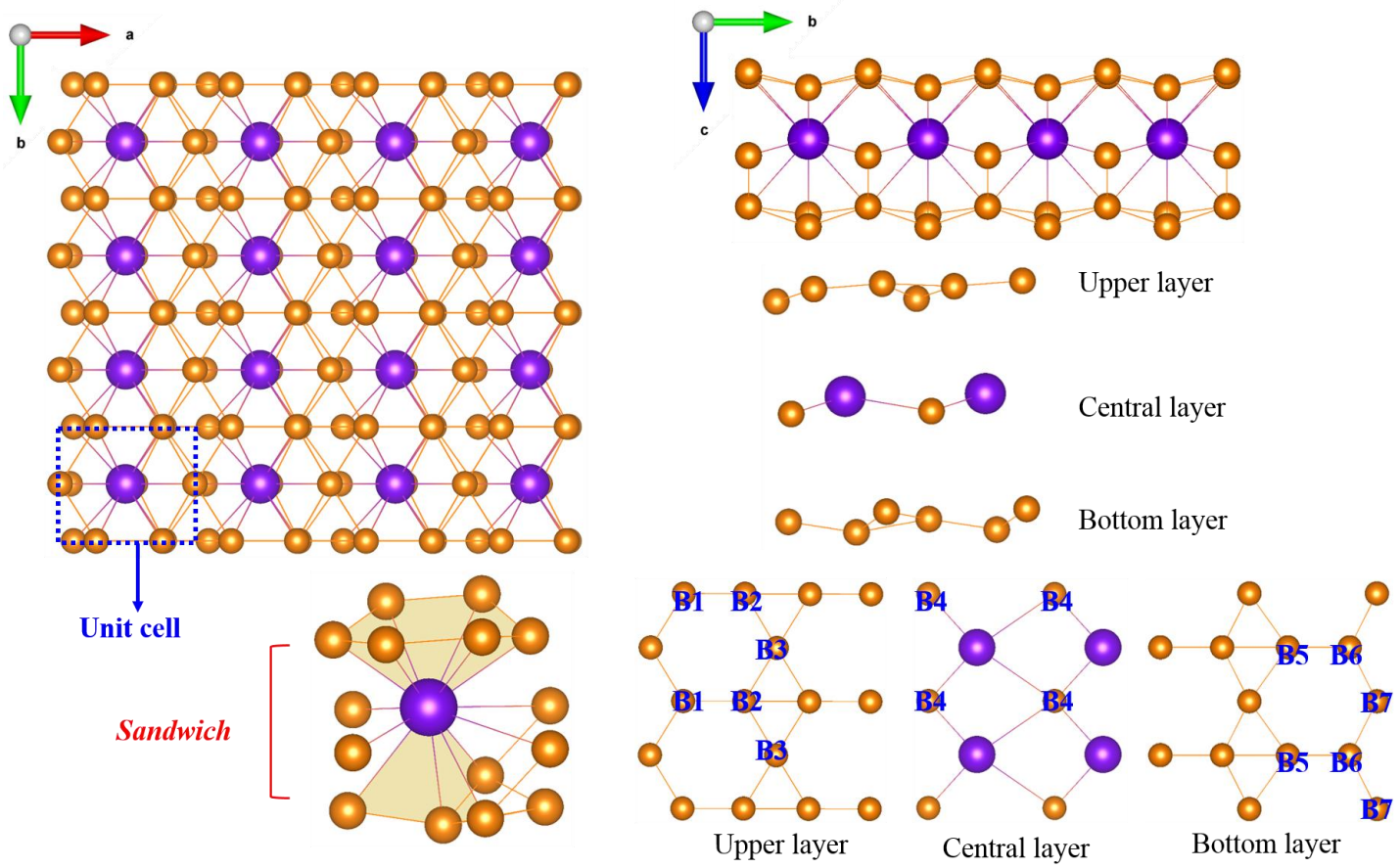

(b)

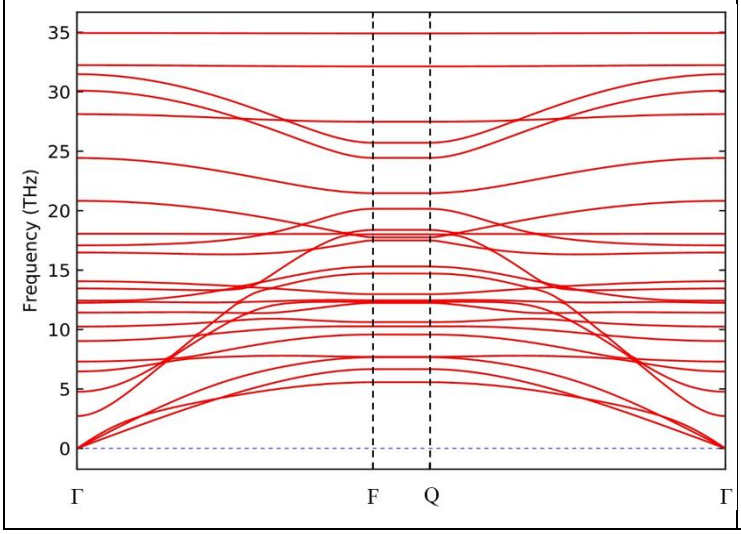

(c)

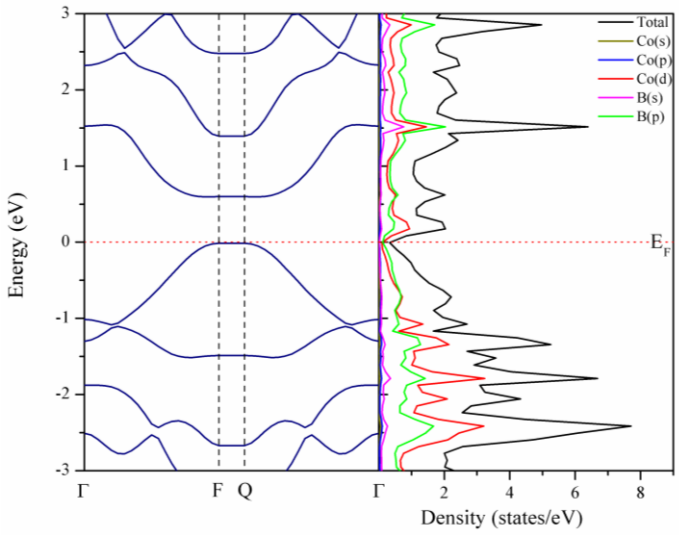

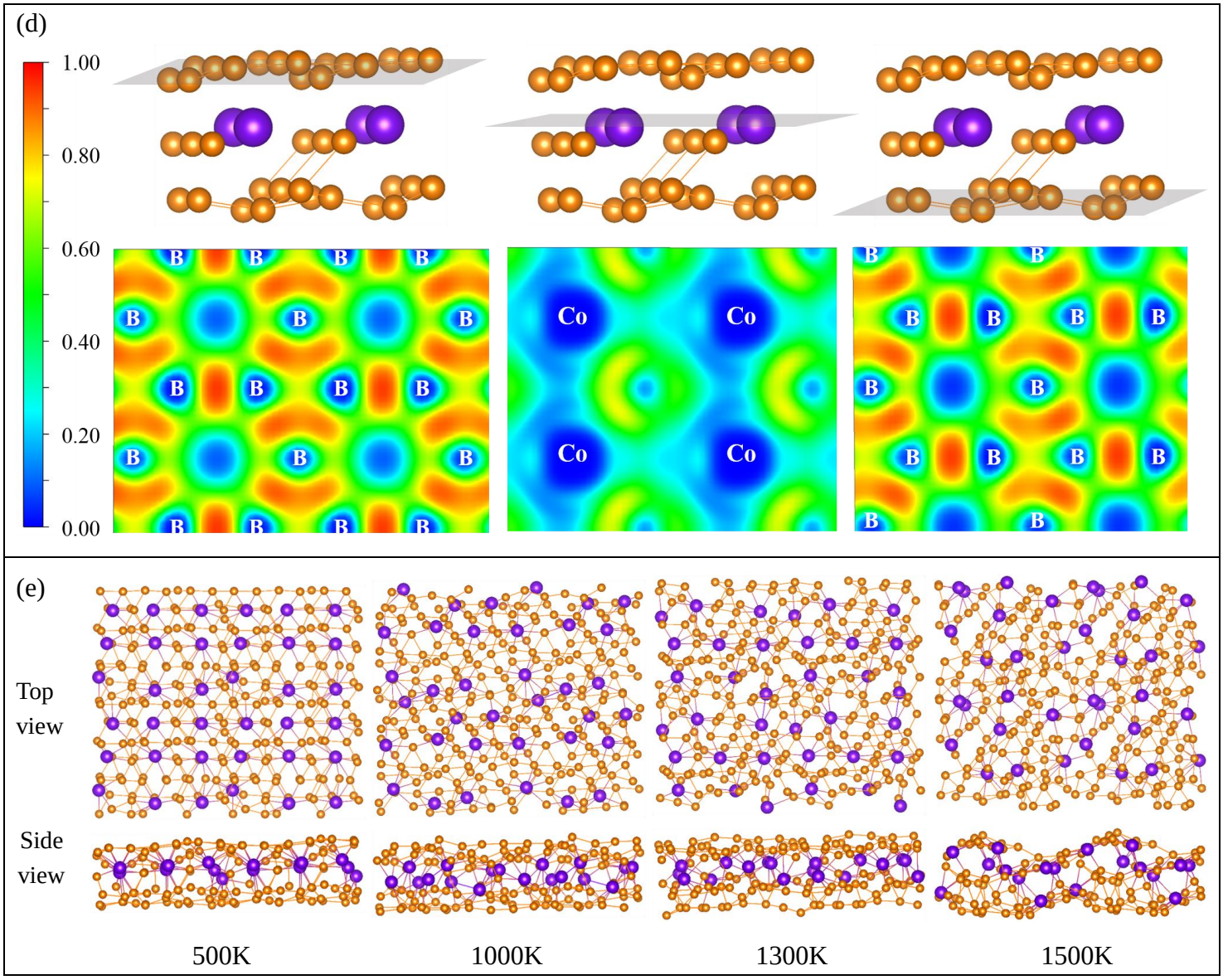

Fig. S1. (a) structural analysis, (b) relative energy, (c) phonon spectra, (d) AIMD simulation results, and (e) electronic properties of the low-lying CoB_7^-i allotropes (i = 2, 3, 4, 6, 7). The relative energy is reference to that of the global minimum CoB_7^-1.

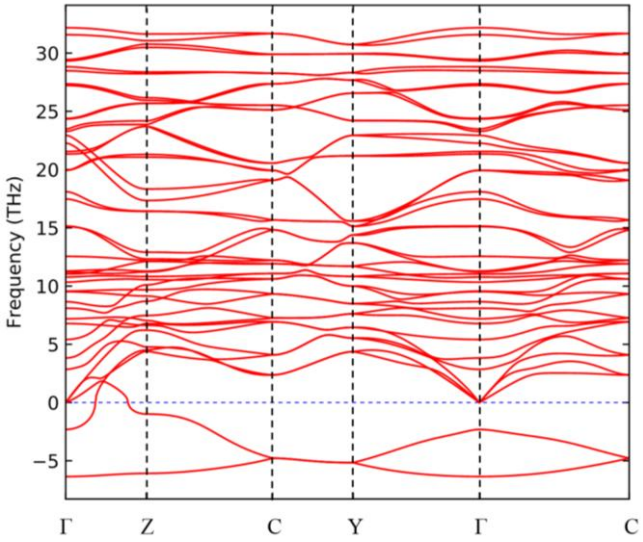

Fig. S2. The phonon spectrum of the boron atomic layer in the CoB_7−1 structure with the Co atom removed.

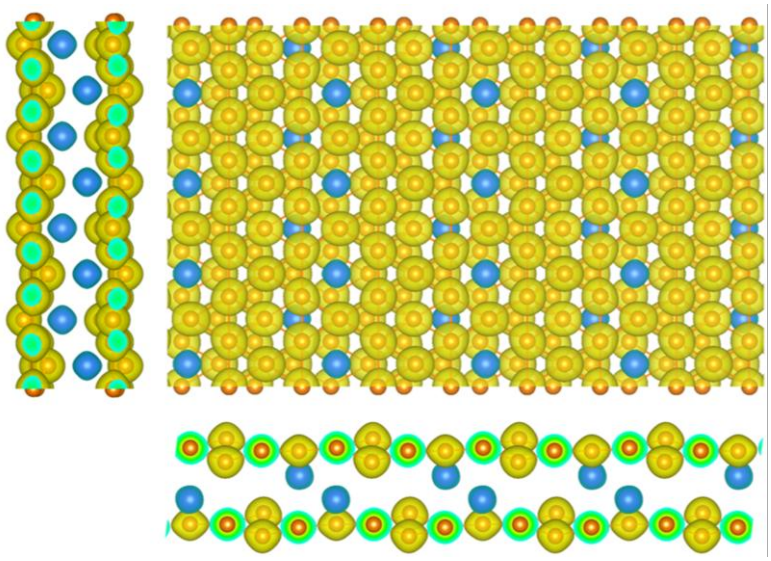

Fig. S3. The Charge density difference plot of the CoB_7−1.

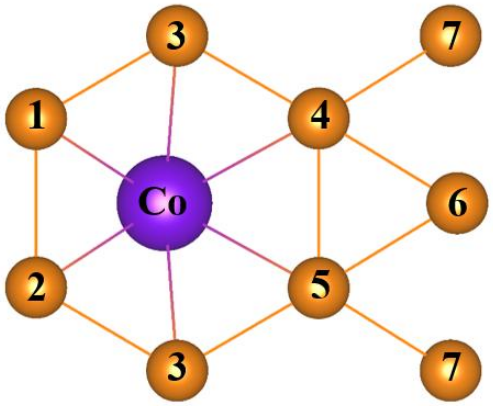

Atom	Charge (e)
Co	-0.0711
B1	-0.0835
B2	-0.0690
B3	+0.0147
B4	+0.0768
B5	-0.0517
B6	+0.0646
B7	+0.1191

Fig. S4. The calculated Bader charges of the CoB_7−1.

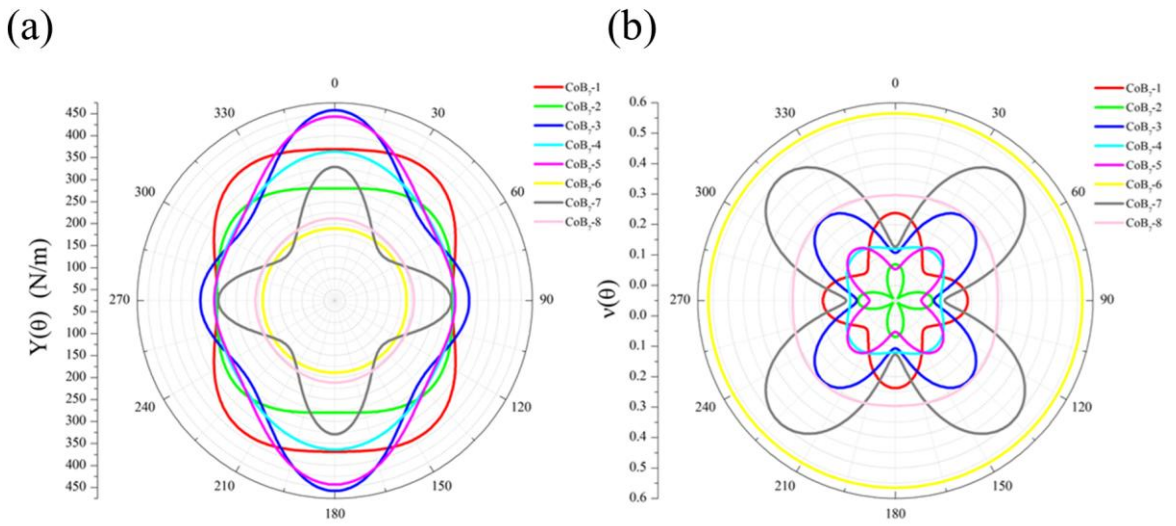

Fig. S5. Polar diagrams of (a) in−plane Young's modules Y(θ) and (b) Poisson's ratio υ(θ) along an arbitrary in−plane direction θ (θ is the angle relative to the x direction) for eight low−lying allotropes (CoB_7−i, i=1−8) of 2D CoB_7 nanosheets.

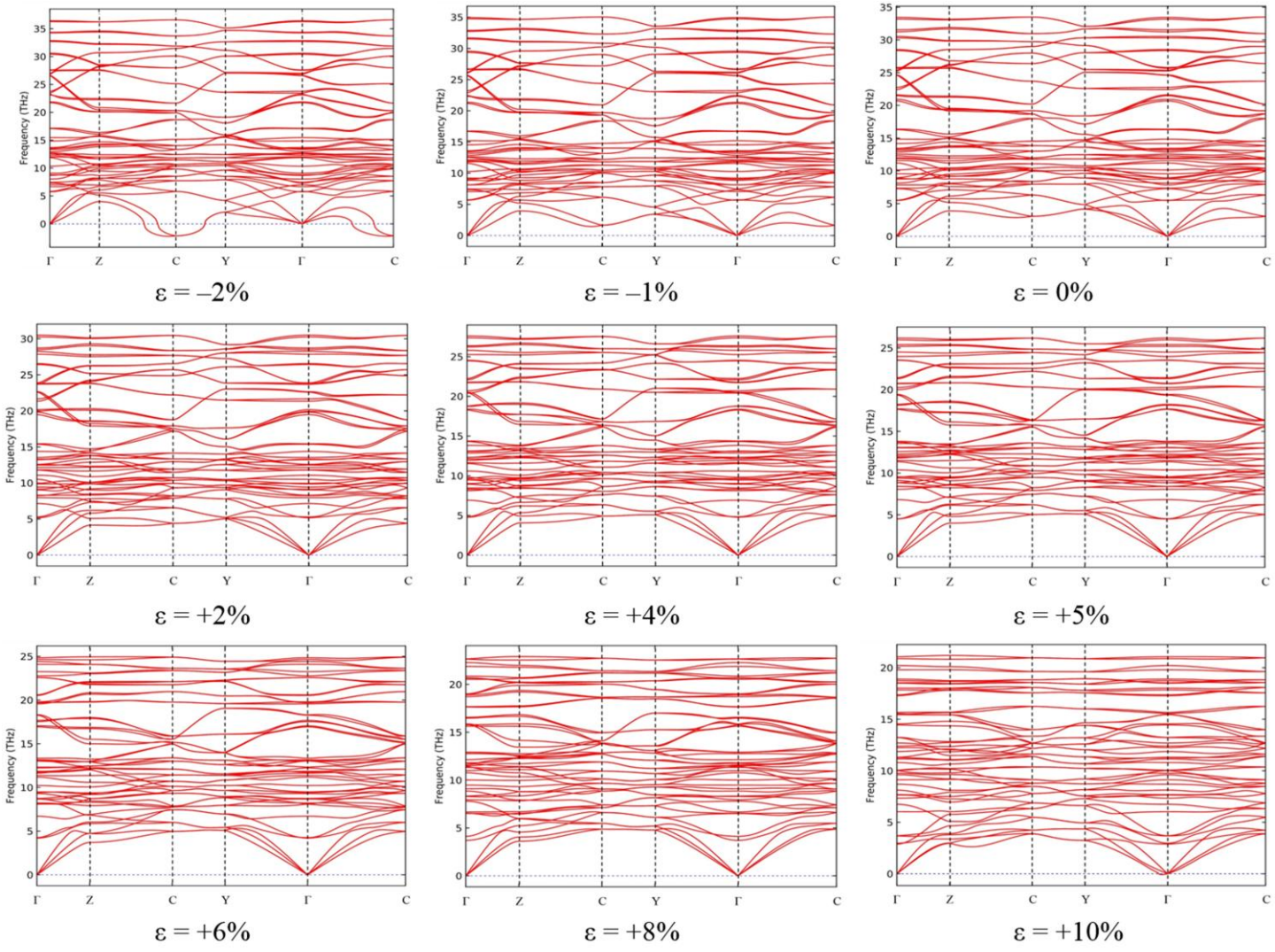

Fig. S6. Phonon dispersion spectra for CoB_7−1 under biaxial strain from −2% to +10%, the stable interval of strain of phonon spectra is −1% ~ +8%.

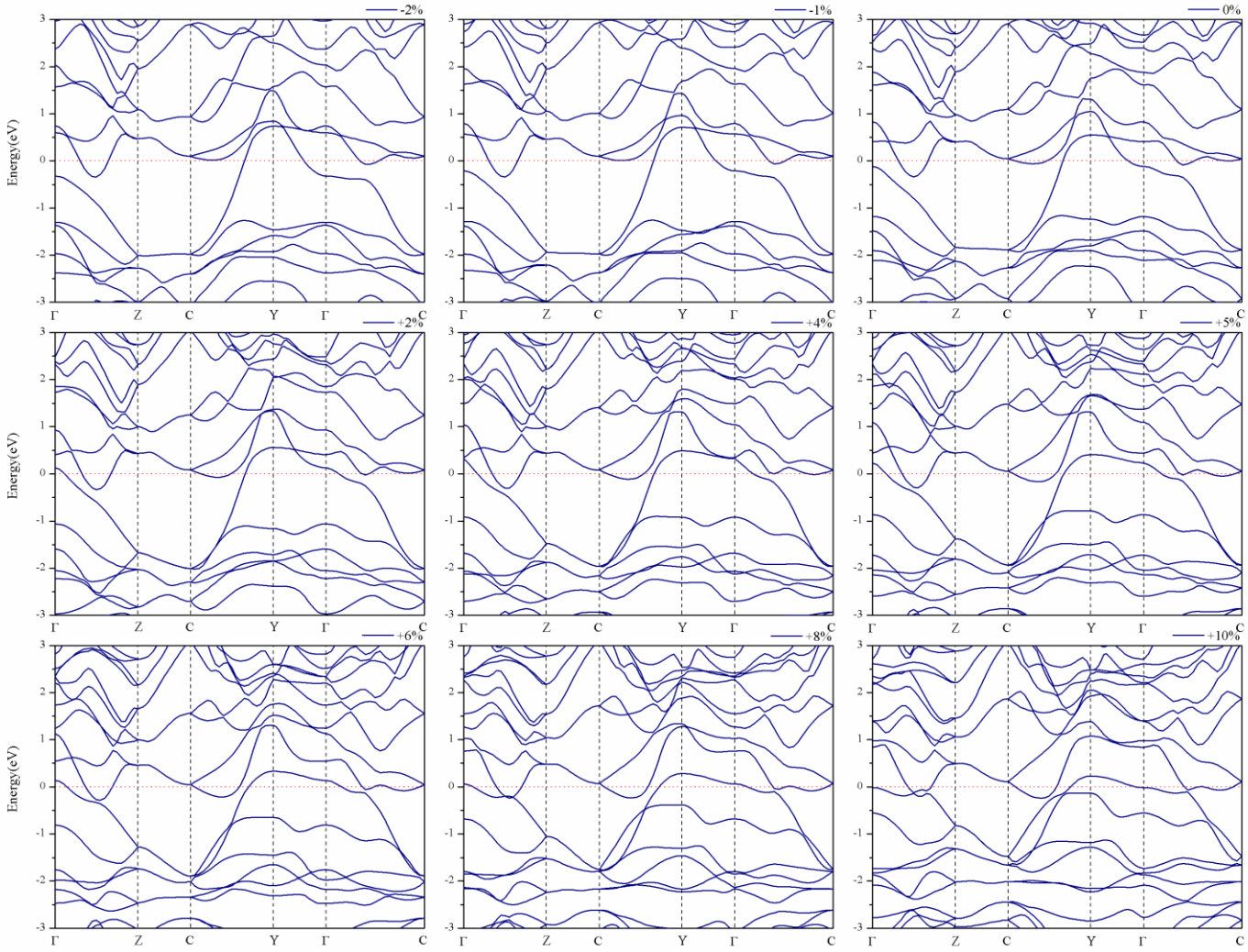

Fig. S7. Electronic band structures of CoB_7−1 under biaxial strain from −2% up to +10%. The Fermi level is set at 0 eV.

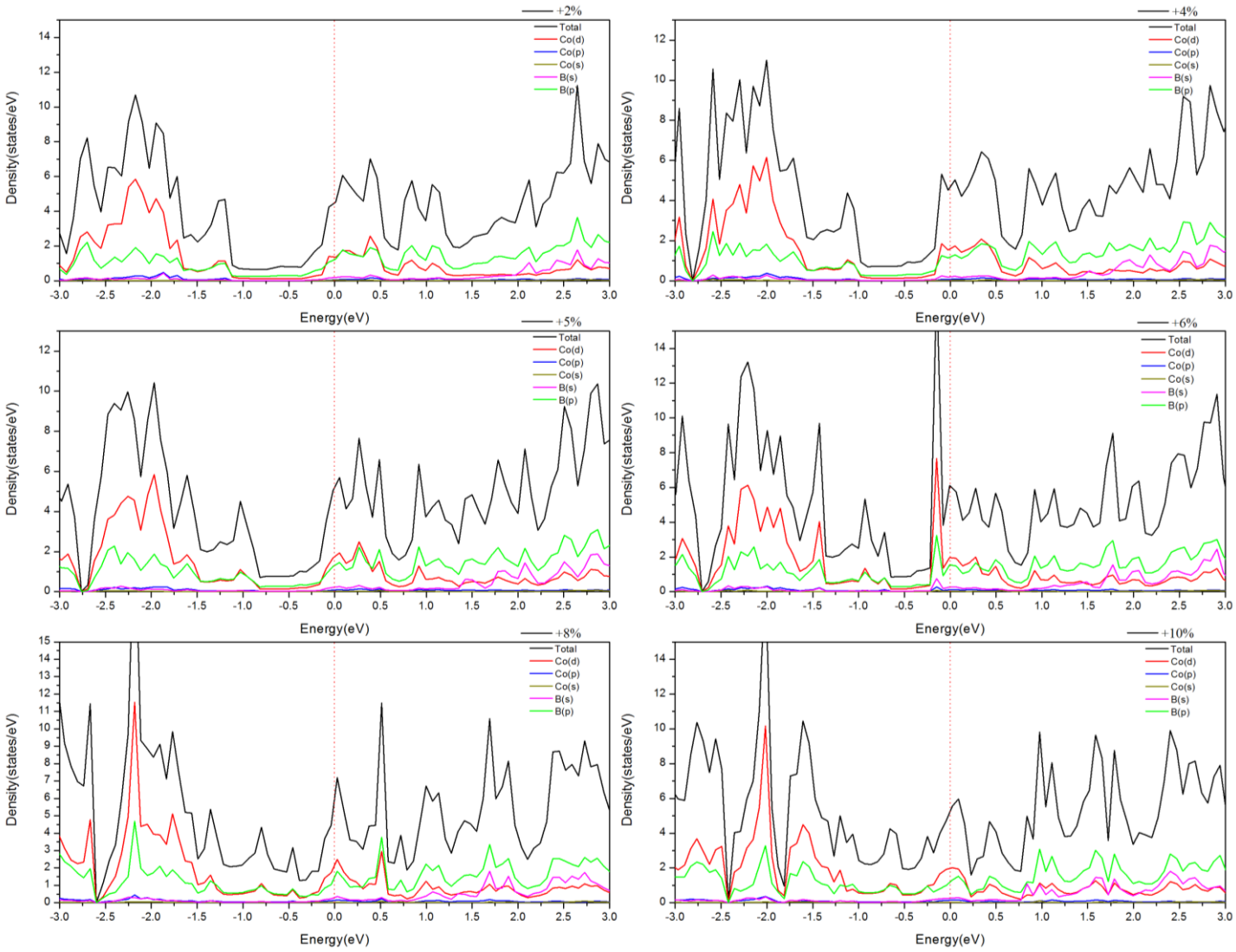

Fig. S8. Density of states of CoB_7−1 under biaxial strain from +2% up to +10%. The Fermi level is set at 0 eV.

Table S1. Elastic constants (C_{ij}, N/m), Layer modulus (γ, N/m), Young's modules (Y, N/m), Poisson's ratio (υ) of seven low−lying allotropes of 2D CoB_7 nanosheets (CoB_7−i), for the easy of comparison, the ground state CoB_7−1 is also listed here, although it has already been discussed in the main text.

CoB_7−i	C_{11}	C_{22}	C_{12}	C_{66}	γ	Young modulus (N/m)		Poisson's ratio	
						Y_x	Y_y	υ_x	υ_y
CoB_7−1	386.1	305.8	72.6	174.7	209.3	368.8	292.1	0.2374	0.1881
CoB_7−2	281.4	294.9	20.4	166.7	154.3	280.0	293.5	0.0693	0.0727
CoB_7−3	461.7	333.9	35.7	112.6	216.7	457.9	331.1	0.1069	0.0773
CoB_7−4	368.1	300.4	36.1	135.6	185.2	363.7	296.9	0.1203	0.0982
CoB_7−5	444.1	299.6	15.8	134.4	193.9	443.3	299.1	0.0528	0.0357
CoB_7−6	277.4	277.4	156.7	60.4	217.0	188.9	188.9	0.5648	0.5648
CoB_7−7	333.8	294.2	37.4	57.9	175.7	329.1	290.0	0.1272	0.1121
CoB_7−8	231.4	224.7	66.5	77.4	147.3	211.7	205.6	0.2961	0.2875